Structure-based discovery of prescription drugs that interact with the norepinephrine transporter, NET

Avner Schlessinger[a,b,c,1], Ethan Geier[a], Hao Fan[a,b,c], John J. Irwin[b,c], Brian K. Shoichet[b,c], Kathleen M. Giacomini[a], and Andrej Sali[a,b,c,1]

[a]Department of Bioengineering and Therapeutic Sciences, [b]Department of Pharmaceutical Chemistry, and [c]California Institute for Quantitative Biosciences, University of California, San Francisco, CA 94158

Edited by Barry Honig, Columbia University, Howard Hughes Medical Institute, New York, NY, and approved July 20, 2011 (received for review April 15, 2011)

The norepinephrine transporter (NET) transports norepinephrine from the synapse into presynaptic neurons, where norepinephrine regulates signaling pathways associated with cardiovascular effects and behavioral traits via binding to various receptors (e.g., β2-adrenergic receptor). NET is a known target for a variety of prescription drugs, including antidepressants and psychostimulants, and may mediate off-target effects of other prescription drugs. Here, we identify prescription drugs that bind NET, using virtual ligand screening followed by experimental validation of predicted ligands. We began by constructing a comparative structural model of NET based on its alignment to the atomic structure of a prokaryotic NET homolog, the leucine transporter LeuT. The modeled binding site was validated by confirming that known NET ligands can be docked favorably compared to nonbinding molecules. We then computationally screened 6,436 drugs from the Kyoto Encyclopedia of Genes and Genomes (KEGG DRUG) against the NET model. Ten of the 18 high-scoring drugs tested experimentally were found to be NET inhibitors; five of these were chemically novel ligands of NET. These results may rationalize the efficacy of several sympathetic (tuaminoheptane) and antidepressant (tranylcypromine) drugs, as well as side effects of diabetes (phenformin) and Alzheimer's (talsaclidine) drugs. The observations highlight the utility of virtual screening against a comparative model, even when the target shares less than 30% sequence identity with its template structure and no known ligands in the primary binding site.

The solute carriers 6 (SLC6) or the sodium:neurotransmitter symporters is a family of ion-dependent transporter proteins that channel neurotransmitters, amino acids, and osmolytes into the cell (1). These transporters regulate a variety of biological activities such as synaptic transmission, neurotransmitter recycling, metabolism, and fluid homeostasis. The norepinephrine or noradrenaline transporter (NET, SLC6A2) is a monoamine transporter mostly expressed in the peripheral and central nervous systems (CNS). NET recycles neurotransmitters, primarily norepinephrine, but also serotonin and dopamine, from synaptic spaces into presynaptic neurons (2, 3). Mutations in NET have been associated with a variety of behavioral disorders, such as attention-deficit hyperactivity disorder (ADHD) and panic disorder, as well as severe orthostatic hypotension (4). Low levels of the NET mRNA and protein have been found in brains of suicidal patients with major depression (4).

NET is a target of drugs treating a variety of mood and behavioral disorders, such as depression, anxiety, and ADHD (4). Many of these drugs inhibit the uptake of norepinephrine into the presynaptic cells through NET (4). These drugs therefore increase the availability of norepinephrine for binding to postsynaptic receptors that regulate adrenergic neurotransmission. NET inhibitors can be specific. For example, the ADHD drug Atomoxetine (Strattera®) is a norepinephrine reuptake inhibitor (NRI) that is highly selective for NET. NET inhibitors can also bind multiple targets, increasing their efficacy as well as their potential patient population. For instance, the antidepressant Venlafaxine (Effexor®) is a serotonin-NRI (SNRI) that targets both NET and the serotonin transporter (SERT, SLC6A4) (4). Because of the lack of high-resolution structural information, most drug discovery efforts targeting NET and other SLC6 transporters, including SERT and dopamine transporter (DAT, SLC6A3), have relied on quantitative structure-activity relationship (QSAR) approaches and pharmacophore modeling (5).

As for other SLC6 family members, NET is predicted to have one domain containing 12 transmembrane helices (2). No structures of human SLC6 members have been determined at atomic resolution; however, the leucine transporter LeuT from the bacterium *Aquifex aeolicus* has been determined by X-ray crystallography in different conformations, with various ligands, including substrates and inhibitors (6). Additional crystallographic and model structures of related transporters (7–11) revealed that the SLC6 family members transport ligands across the cell membrane via the "alternating access" transport mechanism (12, 13). The structures of LeuT in complex with different amino acid ligands suggested a competitive inhibition mechanism (14). In particular, for a substrate to be transported efficiently, it needs to bind to the binding site on the transporter surface as well as fit within the binding cavity of the "occluded" transporter state (14); in contrast, a competitive inhibitor binds to the binding site, but is too large to fit into the binding cavity of the occluded state and thus is not transported through the transporter. In addition to the primary binding site (S1 site), the family members may have additional binding sites such as the clomipramine-binding site on LeuT (6, 15).

Here, we identify approved and "natural" drugs that inhibit NET, using comparative protein structure modeling and virtual ligand screening against the primary binding site, followed by experimental testing of predicted ligands. The ability of these results to explain efficacy and side effects that may result from NET inhibition are considered, as is the potential use of our approach for discovering ligands of other membrane transporters.

Results

Model of NET Binding Site and Its Assessment. NET was modeled based on the structure of the leucine transporter LeuT from *Aquifex aeolicus* (Fig. 1*A* and Figs. S1 and S2). The comparative model contains the whole transmembrane domain, including the 12 transmembrane helices, and the residues comprising the primary binding site (Figs. S1 and S2). The binding site model was assessed by its ability to discriminate between known ligands and likely nonbinders ("decoys") using two measures (Fig. 1*B* and Table S1) (16, 17).

Author contributions: A. Schlessinger, E.G., J.J.I., B.K.S., K.M.G., and A. Sali designed research; A. Schlessinger, E.G., and H.F. performed research; A. Schlessinger, E.G., H.F., J.J.I., B.K.S., K.M.G., and A. Sali contributed new reagents/analytic tools; A. Schlessinger, E.G., H.F., J.J.I., B.K.S., K.M.G., and A. Sali analyzed data; and A. Schlessinger and A. Sali wrote the paper.

The authors declare no conflict of interest.

This article is a PNAS Direct Submission.

[1]To whom correspondence may be addressed. E-mail: schles@salilab.org or sali@salilab.org.

This article contains supporting information online at www.pnas.org/lookup/suppl/doi:10.1073/pnas.1106030108/-/DCSupplemental.

First, we calculated the enrichment factor (EF_n)—the fraction of the annotated ligands among the n top-scoring docking hits compared to their fraction in the entire docking database that includes both ligands and decoys (Eq. **S1**). In particular, we computed the early-stage enrichment factor at 1% of the database (EF_1) as well as the late-stage enrichment factor at 20% of the database (EF_{20}) (Table S1) (16–18). Our refined model obtained the highest enrichment scores among all models (EF_1 of 13.5 and EF_{20} of 3.2; Table S1), even though the enrichment value was not considered during its refinement. These enrichment factor values are consistent with a relatively accurately modeled binding site (16).

Second, we calculated the logarithm of the area under the enrichment curve as a measure for docking accuracy (log AUC; Eq. **S2**, Fig. 1*B*, and Table S1) (16–18). A random selection of compounds from the mixture of actual ligands and decoys yields the log AUC of 14.5. Again, our refined model received the highest enrichment score among all models (log AUC of 37.6; Table S1). As for the enrichment factor values above, such a log AUC value suggests that the model is suitable for selecting ligands for experimental testing (16).

The significance of the observed enrichment factors and log AUC values can also be appreciated by comparing them with the corresponding values for docking of the NET ligand to the LeuT template structure. As expected from the dissimilar binding profiles of the primary binding sites in NET and LeuT (i.e., monoamine neurotransmitters and leucine, respectively), the enrichment of NET ligands yielded by the template (log AUC of 14.7 and EF_{max} of 1.6) was comparable to that of random selection (Fig. 1*B* and Table S1).

Mode of NET-Ligand Interaction. The modeled binding site of NET is small, thus limiting the size of the ligands and their binding modes (Fig. 1 and Figs. S2 and S3). Moreover, the binding site consists of several hydrophobic residues that may contribute to an increased binding affinity via van der Waals interactions with the ligand and the hydrophobic effect. For example, Ala145 and Val148 are predicted to allow for a hydrophobic effect with the aryl portion of norepinephrine (Figs. 1 and 2). Previous studies of SERT showed that its residues at the corresponding positions (i.e., Ala169 and Ile172) also allow for a similar hydrophobic effect with its natural substrate 5-HT (19).

In addition, several polar interactions occur in the model of the NET-ligand complexes (Figs. 1*A* and 2). The modeled Phe72 forms π-cation interactions with norepinephrine via its benzyl side chain, and a hydrogen bond via the amide oxygen of its main chain; oxygen atom of Ala145 makes a hydrogen bond with the catechol group of norepinephrine (Fig. 1*A*); the side chain of Asp75 makes ionic interactions with the amine group of norepinephrine (Fig. 1*A*). The corresponding aspartate residues in the other two human SLC6 monoamine transporters [Asp79 in DAT (20) and Asp98 in SERT (19)] are also predicted to make similar critical interactions with their ligands. The model of SERT suggests that this aspartate forms an ionic interaction with the sodium ion "Na1", adopting a conformation that cannot be ruled out for NET (19).

Virtual Screening of Drugs. The refined model of NET was computationally screened against a library of known drugs from the Kyoto Encyclopedia of Genes and Genomes (KEGG DRUG) database (21), filtered for molecules that are suitable for ligand docking (*SI Text*). The filtered set included 6,436 molecules, including drugs that are marketed in Europe, Japan, and the United States, as well as natural drugs and traditional Chinese medicines. Interestingly, several compounds that were ranked highly in our screen have been shown previously to bind NET. For example, the hypotension drug metaraminol (no. 1 hit) (22) and the nasal decongestants ephedrine (no. 2) (23) are well-characterized NET ligands. In our model, these molecules and other top hits have similar binding modes to that of norepinephrine (Fig. S4), interacting via key NET residues conserved among the monoamine transporters. For example, the norephedrine amine group forms ionic interactions with the side chain of Asp75, and its aromatic ring interacts with the aromatic rings of Phe72, Tyr152, and Phe317. The correct identification of drugs known to interact with NET increases our confidence in the NET binding site model and therefore also in newly predicted ligands, similarly to the correct identification of known substrates (above).

The 200 highest-ranked drugs (the top 3.1% of the drug library) were analyzed manually for the similarities of their predicted poses to those in structurally defined complexes, frequent scaffolds, and common pharmacological function (Dataset S1) (24, 25). For example, the drug tuaminoheptane was ranked no. 18. The pose of tuaminoheptane was similar to the pose of known ligands, such as norepinephrine (Fig. 2*E*). Moreover, tuaminoheptane is chemically similar to other top hits, such as octodrine, heptaminol, and milacemide (hits nos. 29, 86, and 122, respectively; Dataset S1), further suggesting that molecules belonging to this chemotype may interact with NET. Finally, tuaminoheptane, which is typically used as a nasal decongestant, is a stimulant of the sympathetic nervous system, similarly to several other known drugs targeting NET, such as pseudoephedrine and ephedrine.

For experimental testing, we excluded drugs that have been already shown to bind NET (*SI Text*). The 18 drugs selected for testing were classified into two groups.

The first "high-confidence" group included five molecules (Tables S2 and S3) that have predicted binding modes nearly identical to that of the natural substrate norepinephrine, interacting with almost all key NET residues (Figs. 1 and 2). These molecules are chemically similar to known NET ligands (Table S2), sharing key pharmacophoric characteristics: They consist of an aromatic ring and a positively charged amine group (5) (Fig. 2*F*). For example, adrenalone, which is a topical nasal decongestant, hemostatic, and vasoconstrictor, is a keton form of the natural substrate epinephrine (Table S2). Adrenalone is chemically similar to known NET ligands [Tanimoto coefficient (Tc) of 0.40 and 0.61 for the EFCP4 and Daylight fingerprints, respectively (*SI Text*); Table S2]. Additionally, similarly to norepinephrine, adrenalone contains an aromatic ring that forms hydrophobic interactions with Phe72, Tyr152, and Phe317, an amine group that forms an ionic bond with Asp75, and a hydroxyl group that forms a hydrogen bond with Ala145.

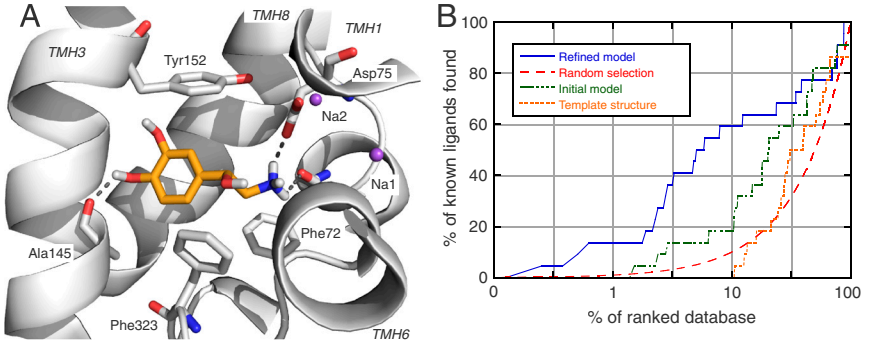

Fig. 1. Validation of modeling and docking. (*A*) Predicted structure of the NET–norepinephrine complex. Norepinephrine is colored in orange, with oxygen, nitrogen, and hydrogen atoms in red, blue, and white, respectively. Sodium ions are visualized as purple spheres. NET's transmembrane helices are depicted as white ribbons. Key residues are displayed as sticks; the three hydrogen bonds between norepinephrine and NET (involving residues Ala145, Phe72, and Asp75) are shown as dotted gray lines. (*B*) Enrichment plots for various structures: the refined NET model (blue), random selection (red), the initial NET model (green), and the LeuT template structure (orange).

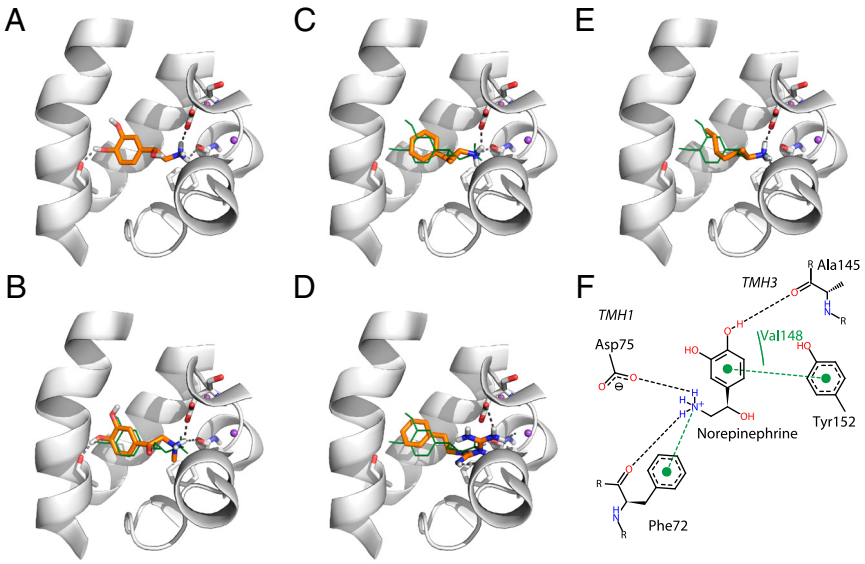

Fig. 2. Predicted binding modes for NET ligands. Predicted binding modes of the known substrate norepinephrine (*A*), and four ligands discovered in the docking screen (*B–E*). Residues making polar interactions with the ligand are illustrated with sticks; carbon atoms are colored in white, nitrogen atoms in blue, and oxygen atoms in red; hydrogen bonds are represented by dotted gray lines. The predicted pose of the known ligand is shown in orange sticks in *A*, and in green lines in *B–E*). The compounds are adrenalone (*B*), tranylcypromine (*C*), phenformin (*D*), and tuaminoheptane (*E*). The proposed key interactions between NET and norepinephrine are highlighted. (*F*) Protein–ligand hydrogen bonds are represented by dashed lines. Hydrophobic effect is represented by green lines. Interactions involving π electrons are represented by dotted green lines.

The second "medium-confidence" group included 13 drugs (Tables S2 and S3). Their predicted binding modes are dissimilar from the binding of the natural substrates. The majority of these drugs have only one of the key pharmacophoric characteristics of the known NET substrates—a polar group that interacts with the key residue Asp75 (Figs. 1 and 2). For example, tuaminoheptane is chemically dissimilar from known NET ligands [Tc of 0.23 (0.18); Table S2]. Tuaminoheptane has an amine group that makes ionic interactions with Asp72 but lacks an aromatic ring to make interactions with the hydrophobic side of the binding site; alternatively, the tuaminoheptane heptane group allows for a hydrophobic interaction with Val148 and Tyr152 (Fig. 2*E*).

Experimental Characterization of Predicted NET Inhibitors. The 18 drugs selected above were tested experimentally for their ability to inhibit [3H]norepinephrine uptake by NET in human embryonic kidney (HEK) cells; desipramine, a known NET inhibitor, served as a positive control (Fig. 3 and Table 1). [3H]norepinephrine uptake was measured in the presence of 10 and 100 μM drug concentrations: Although many drugs are therapeutically dosed to plasma levels of approximately 10 μM, they can potentially reach concentrations as high as 100 μM or greater in the peripheral tissues. In addition, for many CNS-acting drugs and endogenous compounds, the values for the inhibition constants (K_i) at their corresponding receptor target sites have been reported at approximately 10 μM, whereas maximal receptor

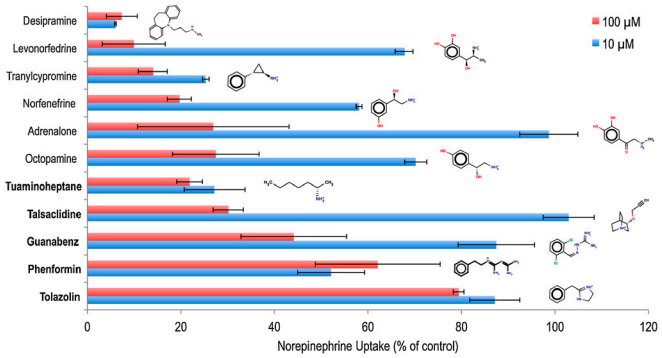

Fig. 3. Uptake experiments. Inhibition of [3H]norepinephrine uptake by the identified inhibitors in NET stable transfected HEK (HEK-NET) cells. HEK-NET cells were incubated with 200 nM unlabeled NE (50 nM radiolabeled [3H] norepinephrine) and either 10 μM (blue) or 100 μM (red) of inhibitor for 3 min. Drugs that are chemically dissimilar to known NET ligands (Table S2) are annotated in bold font.

inhibition can be achieved at 100 μM for many compounds (26). The potencies observed at 10-μM concentration ranged from 75% inhibition (tranylcypromine) to no inhibition (e.g., metformin); the potencies at 100-μM concentrations ranged from 90% (levonordefrin) to no inhibition (e.g., 6-mercaptopurine).

All high-confidence hits exhibited a significant level of inhibition: Substrate uptake by NET was reduced to 25% (14%), 68% (10%), 58% (20%), 99% (27%), and 70 (28%) at 10-μM (100-μM) concentrations of tranylcypromine, levonordefrin, norfenefrine, adrenalone, and octopamine, respectively (Fig. 3 and Table 1); the half maximal inhibitory concentration (IC_{50}) value of tranylcypromine was 8.7 μM (Fig. 4 and Table 1). Supporting these results, levonordefrin interaction with NET was also found to be documented in the DrugBank database (27).

Several medium-confidence hits also exhibited a significant level of inhibition: Substrate uptake by NET was reduced to 87% (44%) and 87% (79%) at 10-μM (100-μM) concentrations

Table 1. Uptake experiments for predicted ligands of NET

Name*	Substrate uptake†, %	IC_{50}‡, μM
High-confidence predictions		
Norfenefrine	58 ± 1 (20 ± 3)	13.9
Levonordefrin	68 ± 2 (10 ± 7)	11.0
Octopamine	70 ± 2 (28 ± 9)	23.6
Tranylcypromine	25 ± 1 (14 ± 3)	8.7
Adrenalone	99 ± 6 (27 ± 16)	36.9
Medium-confidence predictions		
Metformin	102 ± 5 (97 ± 10)	N/A§
Tuaminoheptane	27 ± 7 (22 ± 3)	3.7
Lamivudine	109 ± 9 (111 ± 6)	N/A
Nicotine	97 ± 12 (102 ± 10)	N/A
Lazabemide	144 ± 46 (112 ± 20)	N/A
6-mercaptopurine	102 ± 8 (106 ± 5)	N/A
Talsaclidine	103 ± 5 (30 ± 3)	43.2
Mafenide	90 ± 9 (90 ± 4)	N/A
Tolazolin	87 ± 5 (79 ± 1)	68.0
Phenformin	52 ± 7 (62 ± 13)	10.9
Guanabenz	87 ± 8 (44 ± 11)	69.6
Aceclidine	115 ± 14 (111 ± 29)	N/A
L-phenylalanine	111 ± 10 (104 ± 11)	N/A

*"Name" is the generic name of the molecule.
†"Substrate uptake" gives the percent of [3H]norepinephrine uptake in the presence of 10 μM (100 μM) drug concentrations relative to that uptake in the absence of drugs (*Materials and Methods* and *SI Text*).
‡"IC_{50}" is the estimated half maximal inhibitory concentration value based on measurement of inhibition of substrate uptake at different concentrations (*Materials and Methods* and *SI Text*)
§N/A, not applicable.

of guanabenz and tolazolin, respectively (Fig. 3 and Table 1). In addition, two of the medium-confidence hits were shown to be potent inhibitors of NET: The uptake of substrate by NET for the antidiabetic drug phenformin and the nasal decongestant tuaminoheptane at concentrations of 10 μM were, respectively, 52 and 27% relative to that of uninhibited NET (Fig. 3 and Table 1). Tuaminoheptane inhibition of NET is further supported by its inhibition of norepinephrine transport into bovine chromaffin cells (28); Furthermore, substrate uptake by NET for the anti-Alzheimer's disease drug talsaclidine at concentration of 100 μM was reduced to 30% relative to that of uninhibited NET. Although the inhibition by talsaclidine was substantial only at relatively high concentrations, the relationship between the pharmacodynamic and pharmacokinetic properties of this drug suggest that this inhibition might also occur in vivo at clinical concentrations ($I_{fu,max}/IC_{50} \approx 0.1$; *SI Text*).

Discussion

Polypharmacology is a phenomenon in which a drug binds multiple rather than a single target with significant affinity (29, 30). The effect of polypharmacology on therapy can be positive (effective therapy) and/or negative (side effects). Positive and/or negative effects can be caused by binding to the same or different subsets of targets; binding to some targets may have no effect. Polypharmacology is observed in the treatment of various disorders in the nervous system, often causing severe side effects. For example, the antischizophrenia drug clozapine binds a variety of serotonergic, dopaminergic, muscarinic, adrenergic, and other receptors that are likely to contribute to its high efficacy; simultaneously, at least some of these interactions also cause serious side effects, including a higher risk of agranulocytosis, seizure, weight gain, and diabetes (30, 31).

Three key findings emerge from our study. First, several sympathetic and antidepressant drugs that target a variety of receptors (e.g., α1-adrenergic receptor) and enzymes [e.g., monoamine oxidase (MAO)] (Table S3), are also inhibitors of NET (Figs. 3 and 4; Table 1 and Table S2), thus likely contributing to the efficacy of these drugs and further suggesting the substantial level of polypharmacology of neuroactive drugs. Second, drugs used for the treatment of diseases that are seemingly unrelated to NET function (e.g., diabetes) also inhibit NET activity (Fig. 3; Table 1 and Table S2). This result may explain some side effects of these drugs (e.g., tachycardia) and suggests that side effects of chemically related drugs, used to treat other diseases (e.g., proguanil for malaria), may also be mediated via NET activity. Third, our virtual screening against a comparative model of NET, a membrane protein sharing only 27% sequence identity with its template structure and no known ligands in the primary binding site (Fig. 1), selectively discriminated known ligands from nonligands (Figs. 2 and 3; Table S1). This suggests that the modeling and docking approach might be useful for identifying unknown interactions between drugs and other membrane transporters and for designing new reagents and leads. We take each of the three key findings in turn.

Explaining Efficacy of Drugs. Our uptake experiments show that several drugs inhibit substrate transport by NET (Fig. 3 and Table 1), suggesting that they might achieve their efficacy in part because of this "off-target" activity. These drugs can be classified into three groups as follows.

The first group includes sympathetic drugs that typically activate the sympathetic nervous system via several mechanisms. They can directly activate postsynaptic adrenergic receptors, inhibit the breakdown of neurotransmitters by enzymes, block the reuptake into the presynaptic cells by transporters, and/or stimulate production and release of catecholamines (32). Virtual screening revealed that various activators (i.e., guanabenz, tolazolin, octopamine, levonordefrin, and norfenefrine) of the sympathetic system, which have well-characterized targets (Table S3), also inhibit substrate uptake by NET (Table 1). Inhibition of norepinephrine reuptake by NET may be a therapeutically enhancing effect of these drugs.

The second group includes sympathetic drugs with unknown mechanism, such as adrenalone. Previous studies showed that adrenalone inhibits the activity of dopamine β-oxidase (33). Because this enzyme catalyzes the conversion of dopamine to norepinephrine, adrenalone is expected to attenuate the adrenergic signal. Here, we show that adrenalone inhibits substrate transport by NET (Fig. 3), thereby amplifying the adrenergic signal. Because the pharmacological effects of adrenalone are related to effects that are associated with stronger adrenergic signal (i.e., nasal decongestion and vasoconstriction), it is conceivable that the increase in norepinephrine concentration via NET inhibition is the major molecular mechanism of adrenalone efficacy.

The third group includes antidepressants with known targets. MAO inhibitors (MAOIs) prevent the breakdown of monoamine neurotransmitters, such as norepinephrine and dopamine, by inhibiting MAO, an enzyme that is responsible for their degradation. Therefore, the availability of these neurotransmitters for activating transmission of signals controlling the mood and behavior is increased. Our finding that the MAOI tranylcypromine is an inhibitor of NET (Figs. 3 and 4; Table 1) has the following three clinical implications: (*i*) polypharmacology may contribute to the efficacy of tranylcypromine; (*ii*) tranylcypromine scaffold might be used for indications that are typically treated by NET reuptake inhibitors and not by MAOIs, such as methylphenidate (Ritalin) for ADHD; (*iii*) orthostatic hypotension, a condition that is linked to malfunctions in NET (34) and is also a side effect of MAOIs (35), might be explained by NET binding to tranylcypromine.

Explaining Side Effects. As illustrated by tranylcypromine, side effects are more likely to occur when a drug displays polypharmacology. Our experiments show that two additional drugs (i.e., phenformin and talsaclidine) inhibit substrate transport by NET (Fig. 3 and Table 1). These drugs cause severe side effects that are similar to those triggered by NET inhibitors, suggesting that NET inhibition by these compounds also occurs in vivo.

Talsaclidine is a muscarinic M1 receptor agonist that was under development for the treatment of Alzheimer's disease. Talsaclidine failed in clinical trials because it triggered dose-limiting side effects (36). For example, in some patients talsaclidine caused symptoms including tachycardia, high blood pressure, nausea, diarrhea, excessive sweating, and palpitation. Although some of these symptoms are likely to be triggered by binding to a variety of targets, including the M2 and M3 receptors, the pharmacodynamic properties of talsaclidine indicate that its inhibition of NET uptake is clinically relevant and might also occur in vivo (Table 1 and *SI Text*) (37). These results further support the hypothesis that talsaclidine effects can be explained by stimulation of both the adrenergic and cholinergic systems (36).

Phenformin is a biguanide drug that is typically used for the treatment of type II diabetes. It lowers the blood glucose concentration by a variety of mechanisms, such as decreasing the absorption of glucose in the intestines (38). The drug is still in use in many countries, including Brazil, China, Greece, Poland, Portugal, and Uruguay. However, phenformin was withdrawn from clinical use in United States in 1978 because it was found to be associated with fatal side effects (39, 40). For some patients, phenformin triggers anorexia and high blood pressure by an unknown mechanism (39). Therefore, phenformin inhibition of substrate uptake by NET can be one cause for these side effects. Furthermore, other drugs that are chemically similar to phenformin, containing biguanide and aromatic ring groups, could trigger related side effects via NET inhibition. For example, the prophylactic antimalarial drug chloroguanide (proguanil), an inhibitor of dihydrofolate reductase that is highly similar to phenformin, causes anorexia in 5% of the patients (http://www.drugs.com/sfx/atovaquone-proguanil-side-effects.html). Conversely, metformin,

another antidiabetic biguanide drug that can trigger lactic acidosis (27), does not cause high blood pressure and anorexia, which is consistent with our observation that it does not affect norepinephrine uptake by NET (Fig. 3 and Table 1). Finally, four other phenformin-like drugs (e.g., the antihypertensive drug moroxydine) (Table S4), whose pharmacological effect (i.e., side effects, efficacy, or both) might be explained by NET binding, were ranked highly by our virtual screening (Dataset S1 and Table S3). One of these predicted drugs (i.e., guanabenz) was experimentally validated and was shown to inhibit substrate uptake by NET (Fig. 3).

Virtual Screening Against NET and Other Transporters. NET ligands can inhibit transport by NET via (*i*) competitive binding resulting in either competitive substrates or competitive inhibitors (e.g., ephedrine) or (*ii*) noncompetitive binding to a NET allosteric site (e.g., venlafaxine) that reduces NET's affinity for the natural substrate. Therefore, one issue in predicting new ligands using the NET model is whether the model approximates an active or inhibited conformation of NET. As a modeling template, we used the structure of LeuT in complex with its natural substrate leucine, which was proposed to represent an active, outward-occluded conformation of LeuT (14). Furthermore, recent studies revealed that different inhibitors stabilize unique LeuT conformations (41–43). Taken together, these studies suggest that virtual screening against a single rigid model of NET may not be able to identify all NET ligands. Nevertheless, the docking screen was able to distinguish between some ligands and nonligands. Five of the 10 experimentally verified NET ligands (guanabenz, tolazolin, talsaclidine, phenformin, and tuaminoheptane) are chemically novel (Table S2). The other five identified ligands are chemically similar to known substrates and bind NET in the micromolar range, as expected for substrates. In contrast, large NET inhibitors, such as some SNRIs and tricyclic antidepressants, do not fit into the binding site of our model and thus were not identified by virtual screening. Therefore, to identify NET interactions with large inhibitors, future studies should screen against NET models that are based on the outward-open conformation structure of LeuT (14). Furthermore, to identify new classes of NET ligands, including both substrates and inhibitors, virtual screening against large sets of lead-like molecules (18) should be combined with the chemical similarity ensemble approach (SEA) (31); SEA can relate proteins based on the chemical similarity among their ligands, thus building cross-target similarity maps that are useful in identifying protein–drug interactions (29).

Membrane transporters are key proteins that control the uptake and efflux of various solutes such as amino acids, sugars, and drugs. They can be drug targets themselves or they can regulate the absorption, distribution, metabolism, and elimination of drugs (37). For example, the organic cation transporter 1 (SLC22A1 or OCT1) regulates the cellular concentration of the antidiabetic drug metformin (44, 45). Because of the difficulty of determining atomic structures of membrane proteins, structures of transporters, particularly from human, are not well represented in the Protein Data Bank (PDB) (46). However, in the past few years, structures of several prokaryotic and eukaryotic membrane transporters have been determined at atomic resolution (47, 48). Despite relatively low sequence similarity between these structures and their human homologs with unknown structures, some of these structures can serve as templates for constructing useful models (47).

If the template structures have similar ligand-binding profiles to those of their homologs with unknown structures, they can be used for virtual screening to identify ligands for these homologs (17). For example, the recent crystal structure of the sodium galactose transporter from *Vibrio parahaemolyticus* (vSGLT) (49) can serve to identify ligands of the human glucose transporters of the SLC5 family, which are emerging antidiabetic targets (50). Conversely, if a template has a dissimilar ligand-binding profile from that of its homolog, virtual screening against the template clearly cannot be used to identify homolog's ligands (17), as is exemplified by the LeuT template and its NET homolog (Fig. 2*B* and Table S1), binding leucine and monoamines, respectively. Nontrivially, however, virtual screening against a refined NET model based on the LeuT template did identify some known and unknown ligands (Figs. 2–4).

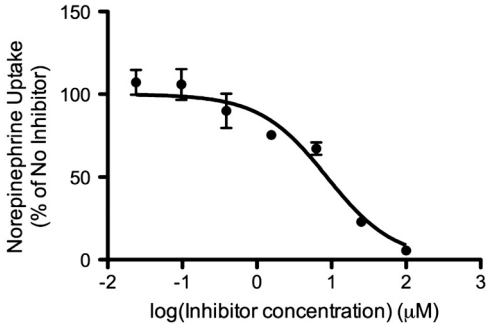

Fig. 4. Uptake kinetic experiment. Concentration-dependent effect of tranylcypromine on [3H]norepinephrine uptake under the same conditions as in Fig. 3. Data are expressed as the percent [3H]norepinephrine uptake in the absence of inhibitor, and are the mean ± standard error of the mean of three independent experiments.

The number of membrane protein structures is expected to grow substantially (51, 52). The combined computational and experimental approach presented in this study is generally applicable to the characterization of transporter structures and their interactions with ligands, including drugs. Thus, it is useful for identifying unknown drug-transporter interactions as well as designing reagents with optimized selectivities.

Materials and Methods

Comparative Model Construction. NET was modeled using MODELLER-10v8 based on the X-ray structure of LeuT from *Aquifex aeolicus* (PDB ID code 2A65) (53) (*SI Text*). The alignment between the NET and LeuT sequences was based on a comprehensive comparison of the SLC6 family members (54) (*SI Text*). The sequence identity between the modeled fraction of NET and LeuT is 27%, covering 77% of NET (Table S1 and Fig. S5. The primary binding site of the initial NET model ("initial model") was refined by repacking the side chains on a fixed backbone using Scwrl4 (55) ("refined model," available in the "Norepinephrine transporter (NET, SLC6A2)" model dataset in ModBase or upon request) (*SI Text*). Individual side chains (i.e., Asp75, Phe72, Tyr152, Phe317, and Ser419) were refined consecutively by Scwrl4, with or without ligand constraints (*SI Text*); Ser419 conformation was refined manually using PyMOL (56). We also tested a NET model ("ModBase") that was based on an automatically computed NET–LeuT alignment downloaded from the ModBase database of annotated comparative protein structure models (Table S1) (57).

Virtual Screening and Ligand Docking. Virtual screening against the NET model was performed using a semiautomatic docking procedure (16, 17, 24, 58), relying on DOCK 3.5.54 (59, 60) (*SI Text*).

Binding Site Assessment. The accuracy of virtual screening was estimated by the enrichment for the known ligands among the top-scoring decoy compounds (61, 62), generated by the Directory of Useful Decoys protocol (16, 18) (*SI Text*).

Cell Lines. Stable transfected HEK293 cells were created by transfecting pcDNA5/FRT (Invitrogen) vector containing the full-length human NET cDNA (HEK-NET) and the empty vector (HEK-EV) using Lipofectamine 2000 (Invitrogen) per manufacturer's instructions. Transfected HEK293 cells were maintained in DMEM-H21 containing 10% FBS, 100 units/mL penicillin, 100 μg/mL streptomycin, and 200 μg/mL hygromycin B at 37 °C in a humidified atmosphere containing 5% CO_2.

Inhibition of Norepinephrine Uptake. Uptake studies were performed as described previously (63). Briefly, cells were seeded at a density of 2×10^5 cells per well in poly-D-lysine-coated 24-well (BD Falcon) plates and were grown to 80–90% confluence. Stable transfected HEK293 cells were rinsed with prewarmed Hanks' balanced salt solution (HBSS) and then incubated in 0.3 mL of prewarmed buffer containing 200 nM unlabeled norepinephrine and 50 nM

radiolabeled [^{3}H]norepinephrine (Perkin Elmer) in the presence and absence of 10 and 100 μM test compound at 37 °C for 3 min. The reaction was terminated by washing cells twice with 1.0 mL of ice-cold HBSS, followed by addition of 700 mL lysis buffer (0.1% SDS wt/vol, 0.1 N NaOH). Intracellular radioactivity was determined by scintillation counting and normalized to per well protein content as measured by using the BCA protein assay (Pierce). Concentration-dependent inhibition for tranylcypromine (Fig. 4) was measured using the same conditions as for the single-point measurements. Cells were incubated with 0.025, 0.1, 0.4, 1.6, 6.25, 25.0, and 100 μM drug concentrations.

ACKNOWLEDGMENTS. We thank Sook Wah Yee, Amber Dahlin, and Keren Lasker for helpful discussions, as well as Ursula Pieper, Ben Webb, and Elina Tjioe for technical assistance and maintenance of the computational resources required for this study. The project was supported by grants from National Institutes of Health (R01 GM54762 to A. Sali, U54 GM094625 and U01 GM61390 to A. Sali and K.M.G., U54 GM093342 and P01 GM71790 to A. Sali and B.K.S., and F32 GM088991 to A. Schlessinger). We also acknowledge funding for computing hardware from Hewlett Packard, IBM, NetApps, Intel, Ron Conway, and Mike Homer.

1. Chen NH, Reith ME, Quick MW (2004) Synaptic uptake and beyond: The sodium- and chloride-dependent neurotransmitter transporter family SLC6. *Pflugers Arch* 447:519–531.
2. Pacholczyk T, Blakely RD, Amara SG (1991) Expression cloning of a cocaine- and antidepressant-sensitive human noradrenaline transporter. *Nature* 350:350–354.
3. Rudnick G, Clark J (1993) From synapse to vesicle: The reuptake and storage of biogenic amine neurotransmitters. *Biochim Biophys Acta* 1144:249–263.
4. Hahn MK, Blakely RD (2007) The functional impact of SLC6 transporter genetic variation. *Annu Rev Pharmacol Toxicol* 47:401–441.
5. Andersen J, Kristensen AS, Bang-Andersen B, Stromgaard K (2009) Recent advances in the understanding of the interaction of antidepressant drugs with serotonin and norepinephrine transporters. *Chem Commun (Camb)* 3677–3692.
6. Nyola A, et al. (2010) Substrate and drug binding sites in LeuT. *Curr Opin Struct Biol* 20:415–422.
7. Kanner BI, Zomot E (2008) Sodium-coupled neurotransmitter transporters. *Chem Rev* 108:1654–1668.
8. Krishnamurthy H, Piscitelli CL, Gouaux E (2009) Unlocking the molecular secrets of sodium-coupled transporters. *Nature* 459:347–355.
9. Abramson J, Wright EM (2009) Structure and function of Na(+)-symporters with inverted repeats. *Curr Opin Struct Biol* 19:425–432.
10. Forrest LR, et al. (2008) Mechanism for alternating access in neurotransmitter transporters. *Proc Natl Acad Sci USA* 105:10338–10343.
11. Shi L, Quick M, Zhao Y, Weinstein H, Javitch JA (2008) The mechanism of a neurotransmitter:sodium symporter—Inward release of Na+ and substrate is triggered by substrate in a second binding site. *Mol Cell* 30:667–677.
12. Jardetzky O (1966) Simple allosteric model for membrane pumps. *Nature* 211:969–970.
13. Guan L, Kaback HR (2006) Lessons from lactose permease. *Annu Rev Biophys Biomol Struct* 35:67–91.
14. Singh SK, Piscitelli CL, Yamashita A, Gouaux E (2008) A competitive inhibitor traps LeuT in an open-to-out conformation. *Science* 322:1655–1661.
15. Piscitelli CL, Krishnamurthy H, Gouaux E (2010) Neurotransmitter/sodium symporter orthologue LeuT has a single high-affinity substrate site. *Nature* 468:1129–1132.
16. Huang N, Shoichet BK, Irwin JJ (2006) Benchmarking sets for molecular docking. *J Med Chem* 49:6789–6801.
17. Fan H, et al. (2009) Molecular docking screens using comparative models of proteins. *J Chem Inf Model* 49:2512–2527.
18. Irwin JJ, Shoichet BK (2005) ZINC—A free database of commercially available compounds for virtual screening. *J Chem Inf Model* 45:177–182.
19. Celik L, et al. (2008) Binding of serotonin to the human serotonin transporter. Molecular modeling and experimental validation. *J Am Chem Soc* 130:3853–3865.
20. Beuming T, et al. (2008) The binding sites for cocaine and dopamine in the dopamine transporter overlap. *Nat Neurosci* 11:780–789.
21. Okuda S, et al. (2008) KEGG Atlas mapping for global analysis of metabolic pathways. *Nucleic Acids Res* 36:W423–W426.
22. Shore PA, Busfield D, Alpers HS (1964) Binding and release of metaraminol: Mechanism of norepinephrine depletion by alpha-methyl-m-tyrosine and related agents. *J Pharmacol Exp Ther* 146:194–199.
23. Rothman RB, et al. (2003) In vitro characterization of ephedrine-related stereoisomers at biogenic amine transporters and the receptorome reveals selective actions as norepinephrine transporter substrates. *J Pharmacol Exp Ther* 307:138–145.
24. Shoichet BK (2004) Virtual screening of chemical libraries. *Nature* 432:862–865.
25. Kuntz ID (1992) Structure-based strategies for drug design and discovery. *Science* 257:1078–1082.
26. Nikolaev VO, Hoffmann C, Bunemann M, Lohse MJ, Vilardaga JP (2006) Molecular basis of partial agonism at the neurotransmitter alpha2A-adrenergic receptor and Gi-protein heterotrimer. *J Biol Chem* 281:24506–24511.
27. Wishart DS, et al. (2006) DrugBank: A comprehensive resource for in silico drug discovery and exploration. *Nucleic Acids Res* 34(Database issue):D668–D672.
28. Delicado EG, Fideu MD, Miras-Portugal MT, Pourrias B, Aunis D (1990) Effect of tuamine, heptaminol and two analogues on uptake and release of catecholamines in cultured chromaffin cells. *Biochem Pharmacol* 40:821–825.
29. Keiser MJ, et al. (2009) Predicting new molecular targets for known drugs. *Nature* 462:175–181.
30. Roth BL, Sheffler DJ, Kroeze WK (2004) Magic shotguns versus magic bullets: Selectively non-selective drugs for mood disorders and schizophrenia. *Nat Rev Drug Discov* 3:353–359.
31. Keiser MJ, et al. (2007) Relating protein pharmacology by ligand chemistry. *Nat Biotechnol* 25:197–206.
32. Leonard BE (2003) *Fundamentals of Psychopharmacology* (John Wiley & Sons, Chichester, UK), 3rd Ed, p 536.
33. Goldstein M, Contrera JF (1961) Inhibition of dopamine beta oxidase by adrenalone. *Nature* 192:1081.
34. Hahn MK, Robertson D, Blakely RD (2003) A mutation in the human norepinephrine transporter gene (SLC6A2) associated with orthostatic intolerance disrupts surface expression of mutant and wild-type transporters. *J Neurosci* 23:4470–4478.
35. Kaludercic N, Carpi A, Menabo R, Di Lisa F, Paolocci N (2010) Monoamine oxidases (MAO) in the pathogenesis of heart failure and ischemia/reperfusion injury. *Biochim Biophys Acta* 1813:1323–1332.
36. Adamus WS, Leonard JP, Troger W (1995) Phase I clinical trials with WAL 2014, a new muscarinic agonist for the treatment of Alzheimer's disease. *Life Sci* 56:883–890.
37. Giacomini KM, et al. (2010) Membrane transporters in drug development. *Nat Rev Drug Discov* 9:215–236.
38. Grodsky GM, Karam JH, Pavlatos FC, Forsham PH (1963) Reduction by phenformin of excessive insulin levels after glucose loading in obese and diabetic subjects. *Metabolism* 12:278–286.
39. Mc KJ, Kuwayti K, Rado PP (1959) Clinical experience with DBI (phenformin) in the management of diabetes. *Can Med Assoc J* 80:773–778.
40. Wise PH, et al. (1976) Phenformin and lactic acidosis. *Br Med J* 1:70–72.
41. Claxton DP, et al. (2010) Ion/substrate-dependent conformational dynamics of a bacterial homolog of neurotransmitter:sodium symporters. *Nat Struct Mol Biol* 17:822–829.
42. Zhao Y, et al. (2010) Single-molecule dynamics of gating in a neurotransmitter transporter homologue. *Nature* 465:188–193.
43. Nyola A, et al. (2010) Substrate and drug binding sites in LeuT. *Curr Opin Struct Biol* 20:415–422.
44. Shu Y, et al. (2007) Effect of genetic variation in the organic cation transporter 1 (OCT1) on metformin action. *J Clin Invest* 117:1422–1431.
45. Shu Y, et al. (2003) Evolutionary conservation predicts function of variants of the human organic cation transporter, OCT1. *Proc Natl Acad Sci USA* 100:5902–5907.
46. Kelly L, et al. (2009) A survey of integral alpha-helical membrane proteins. *J Struct Funct Genomics* 10:269–280.
47. Schlessinger A, et al. (2010) Comparison of human solute carriers. *Protein Sci* 19:412–428.
48. He X, et al. (2010) Structure of a cation-bound multidrug and toxic compound extrusion transporter. *Nature* 467:991–994.
49. Faham S, et al. (2008) The crystal structure of a sodium galactose transporter reveals mechanistic insights into Na+/sugar symport. *Science* 321:810–814.
50. Wright EM, Hirayama BA, Loo DF (2007) Active sugar transport in health and disease. *J Intern Med* 261:32–43.
51. Stroud RM, et al. (2009) 2007 Annual progress report synopsis of the Center for Structures of Membrane Proteins. *J Struct Funct Genomics* 10:193–208.
52. Love J, et al. (2010) The New York Consortium on Membrane Protein Structure (NYCOMPS): A high-throughput platform for structural genomics of integral membrane proteins. *J Struct Funct Genomics* 11:191–199.
53. Yamashita A, Singh SK, Kawate T, Jin Y, Gouaux E (2005) Crystal structure of a bacterial homologue of Na+/Cl−-dependent neurotransmitter transporters. *Nature* 437:215–223.
54. Beuming T, Shi L, Javitch JA, Weinstein H (2006) A comprehensive structure-based alignment of prokaryotic and eukaryotic neurotransmitter/Na+ symporters (NSS) aids in the use of the LeuT structure to probe NSS structure and function. *Mol Pharmacol* 70:1630–1642.
55. Krivov GG, Shapovalov MV, Dunbrack RL, Jr (2009) Improved prediction of protein side-chain conformations with SCWRL4. *Proteins* 77:778–795.
56. DeLano WL (2002) *The PyMOL Molecular Graphics System* (DeLano Scientific, San Carlos, CA).
57. Pieper U, et al. (2011) ModBase, a database of annotated comparative protein structure models, and associated resources. *Nucleic Acids Res* 39:D465–D474.
58. Irwin JJ, et al. (2009) Automated docking screens: A feasibility study. *J Med Chem* 52:5712–5720.
59. Lorber DM, Shoichet BK (2005) Hierarchical docking of databases of multiple ligand conformations. *Curr Top Med Chem* 5:739–749.
60. Mysinger MM, Shoichet BK (2010) Rapid context-dependent ligand desolvation in molecular docking. *J Chem Inf Model* 50:1561–1573.
61. Cavasotto CN, et al. (2008) Discovery of novel chemotypes to a G-protein-coupled receptor through ligand-steered homology modeling and structure-based virtual screening. *J Med Chem* 51:581–588.
62. Evers A, Gohlke H, Klebe G (2003) Ligand-supported homology modelling of protein binding-sites using knowledge-based potentials. *J Mol Biol* 334:327–345.
63. Chen Y, Zhang S, Sorani M, Giacomini KM (2007) Transport of paraquat by human organic cation transporters and multidrug and toxic compound extrusion family. *J Pharmacol Exp Ther* 322:695–700.